Received: 14 February 2023 | Revised: 25 April 2023 | Accepted: 17 May 2023

DOI: 10.1096/fba.2023-00011

RESEARCH ARTICLE

FASEB BioAdvances WILEY

An insight on the *N*-glycome of notochordal cell-rich porcine nucleus pulposus during maturation

Büşra Günay[1] | **Elizabeth Matthews**[2] | **Jack Morgan**[2] | **Marianna A. Tryfonidou**[3] | **Radka Saldova**[2,4] | **Abhay Pandit**[1]

[1]CÚRAM SFI Research Centre for Medical Devices, University of Galway, Galway, Ireland

[2]NIBRT GlycoScience Group, National Institute for Bioprocessing Research and Training (NIBRT), Dublin, Ireland

[3]Faculty of Veterinary Medicine, Department of Clinical Sciences, Utrecht University, Utrecht, The Netherlands

[4]School of Medicine, College of Health and Agricultural Science, University College Dublin, Dublin, Ireland

Correspondence
Abhay Pandit, SFI Research Centre for Medical Devices, University of Galway, Galway, Ireland, Ireland.
Email: abhay.pandit@universityofgalway.ie

Radka Saldova, NIBRT GlycoScience Group, National Institute for Bioprocessing Research and Training (NIBRT), Dublin, Ireland.
Email: radka.fahey@nibrt.ie

Abstract

Degeneration of the intervertebral disc is an age-related condition. It also accompanies the disappearance of the notochordal cells, which are remnants of the developmental stages of the nucleus pulposus (NP). Molecular changes such as extracellular matrix catabolism, cellular phenotype, and glycosaminoglycan loss in the NP have been extensively studied. However, as one of the most significant co- and posttranslational modifications, glycosylation has been overlooked in cells in degeneration. Here, we aim to characterize the *N*-glycome of young and mature NP and identify patterns related to aging. Accordingly, we isolated *N*-glycans from notochordal cell-rich NP from porcine discs, characterized them using a combined approach of exoglycosidase digestions and analysis with hydrophilic interaction ultra-performance liquid chromatography and mass spectrometry. We have assigned over 300 individual *N*-glycans for each age group. Moreover, we observed a notable abundance of antennary structures, galactosylation, fucosylation, and sialylation in both age groups. In addition, as indicated from our results, increasing outer arm fucosylation and decreasing α(2,3)-linked sialylation with aging suggest that these traits are age-dependent. Lastly, we have focused on an extensive characterization of the *N*-glycome of the notochordal cell-rich NP in aging without inferred degeneration, describing glycosylation changes specific for aging only. Our findings in combination with those of other studies, suggest that the degeneration of the NP does not involve identical processes as aging.

KEYWORDS

aging, intervertebral disc degeneration, liquid chromatography-mass spectrometry, *N*-glycosylation, notochordal cells, nucleus pulposus

Radka Saldova and Abhay Pandit joint authorship.

1 | INTRODUCTION

Intervertebral disc (IVD) degeneration occurs due to the aging of the IVD itself, starting with the inner nucleus pulposus (NP) failing to keep its water retention capabilities. The NP cells lose their viability, extracellular matrix (ECM) production reduces while metalloproteases (MMPs) take over, leading to tissue catabolism. These changes radiate to the outer annulus fibrosus; when it is unable to compensate, these changes lead to structural deterioration and ultimately present in the clinic as IVD-related lower back pain.[1]

In the context of the IVD, aging has been a rather confounding factor making it difficult to understand its degeneration. NP is a very primitive tissue in that it is developmentally derived from the notochord. It is not known what exactly causes NP formation from the notochord; however, as reviewed by Lawson and Harfe, it is suggested that the notochordal cells are either "pushed" toward the regions that eventually form NP, or migrate through the attraction/repulsion of proteins.[2] The largely vacuolated notochordal cell (NC) remnants that initially reside within the core of the IVD can produce high amounts of ECM abundant in glycosaminoglycans (GAGs).[3,4] These cells disappear with adulthood but can be found in the NP until about 10 years of age in humans. This is thought to coincide with the transitional changes in the IVD; whether this is a natural course of maturation or a precursor of the disease, NCs transition into non-vacuolated chondrocyte-like cells forming what is termed NP cells that are functionally and phenotypically different from each other.[5] It is suggested that this transition includes changes in the hydrostatic pressure, osmolarity, and mechanical regulation.[6–8] Unlike humans, there are species including pigs, rats, and non-chondrodystrophic dogs[9] that do not lose this unique population of cells and, incidentally, do not suffer from spontaneous IVD degeneration. Whether this is indeed a result of the NC presence is yet to be proven.

Maintaining NCs' phenotype in vitro to study their involvement is necessary yet challenging.[10,11] In studies to overcome this issue, conditioned media derived from the NC-rich NP tissue implicated the NCs' capability to induce rejuvenating effects on discs and cells.[12–14] Bach et al. found that in a large animal model of disc degeneration, notochordal cell-derived matrix had regenerative effects on the disc, increasing the glycosaminoglycan and ECM production.[15] Other studies followed these investigations on secretome and proteome analysis of NCs as recently reviewed.[16] A number of proteins and soluble factors, including major signaling components such as connective tissue growth factor and transforming growth factor beta 1 were identified in the secretome from notochordal cell-derived conditioned medium.[17]

However, one of the most essential aspects of omics, glycosylation, has universally been neglected in the IVD field. Many proteins and lipids including the cells' very own membrane are highly glycosylated. Glycosylation patterns take shape at the endoplasmic reticulum and are carried and incorporated into proteins via large families of glycosyltransferases. It is a dynamic network allowing the crosstalk among cells, correct conformation of the proteins, signal transduction and other factors. *N*-linked glycans, named so due to their glycosidic bond at the nitrogen of the asparagine in the peptide, are the most abundant (90% of eukaryotic glycoproteins) glycosylation type.[18] *N*-glycosylation is a co-translational mechanism driven without a template, in contrast to proteins. This creates heterogeneity in the glyco-conjugates, making it challenging to assign well-defined functions to the glycans themselves. The complexity of the glycosylation comes not only from the variety of combinations of the saccharides but also from such decorations described as sulfation, acetylation and other modifications. These can be regulated by intrinsic or extrinsic factors and can have radical impacts such as pro-apoptotic effects.[19,20]

There is a lack of complete understanding regarding disease mechanisms; nevertheless, there have been reports suggesting the involvement of certain glycosylation patterns in the diseased tissues. For example, a decrease in α(2,3)-linked monosialylation and total fucosylation has been reported in an LPS-induced neuroinflammation model in the rodent brain.[21] Fucosylation has also been found to interfere with TGFβ-1 signaling, MMP expression and ECM production.[22] Moreover, a decrease in galactosylation, α(2,3) and α(2,6) sialylation, accompanied by increased fucosylation have been reported in serum proteins from patients with multiple myeloma.[23] Many diseases develop with age and maturation; and it is reported that some nongalactosylated and core fucosylated biantennary glycans from serum, plasma, and other body fluids were related simply to the age of the individual.[24] It is evident that glycosylation and its modifications can be an indicator of changes in the biological status. Consequently, changes in glycosylation patterns can also provide considerable information as to the causes of degeneration.

In this study, we hypothesized that the notochordal cell-rich NP would have a distinct *N*-glycome, yet start diverging with maturation. For this purpose, normal NP tissue from young growing pigs and from adult pigs was used in our analysis (Figure 1). This complete *N*-glycome characterization, having not been reported before, gives a better understanding to the glycomic changes that occur during early aging of the NP represented here by the two age-groups studied, and allows therapeutic targets for intervertebral disc degeneration to be identified and utilized effectively.

2 | EXPERIMENTAL PROCEDURES

2.1 | Chemicals and reagents

Sodium dodecyl sulfate (SDS), N,N,N,N′-Tetramethylethylenediamine (TEMED), acetonitrile (ACN), dithiothreitol (DTT), iodoacetamide (IAA), formic acid, 2-aminobenzamide (2-AB), sodium cyanoborohydride (NAB_3CN), dimethyl sulfoxide (DMSO) were purchased from Sigma Aldrich. Other materials used were Tris-HCl (AnalaR, VWR 441514A), Protogel (National Diagnostics, Hessle, Hull, UK, EC-890), ammonium peroxisulphate (APS, AnalaR; BDH 100323W), $NaHCO_3$ (Merck, EM-SX0320-1), peptide-*N*-glycosidase F (PNGaseF, 500,000 units/mL, New England Biolabs, P0709L), AcroPrep Advance 96 filter plate (Pall Life Sciences, PN 8231, 1 µm Glass Fiber, 2 mL well, NTRL), polypropylene 2 mL deep 96well blocks (X50 Microplate, 96 square well, 2 mL, Fisher Scientific, 11511963), 1,2-diamino4,5-methylenedioxybenzene (DMB, Ludger Ltd., LudgerTag DMB kit: LT-KDMB-A1), cOmplete™ protease inhibitor cocktail (Roche, 04693132001).

2.2 | Tissue procurement

Cryopreserved porcine spine segments were procured from mix-breed pigs that were euthanized for unrelated reasons, and kindly provided by Utrecht University. Randomly selected six discs among L2-3, L4-5, and L5-6 levels from six piglets (6 weeks old, 7–10 kg) and five discs from two adult pigs (2 years old, 250–300 kg) were used in the study. Nucleus pulposus (NP) of the IVDs were isolated upon thawing using a sterile scalpel and collected in a tube per age group for homogenization and downstream analysis (Figure 1).

2.3 | Glycoprotein extraction, *N*-glycan release, and 2-AB labeling

Collected NP tissue was homogenized with an 8 mm stainless steel bead using an automated homogenizer (Qiagen TissueLyser LT) at 50/s for 2 h (at 4°C) in TRIS-SDS-based lysis buffer (0.5 M Tris, pH 6.6, 2% SDS) with protease inhibitor cocktail (1x, according to the manufacturer's protocol). The supernatant containing

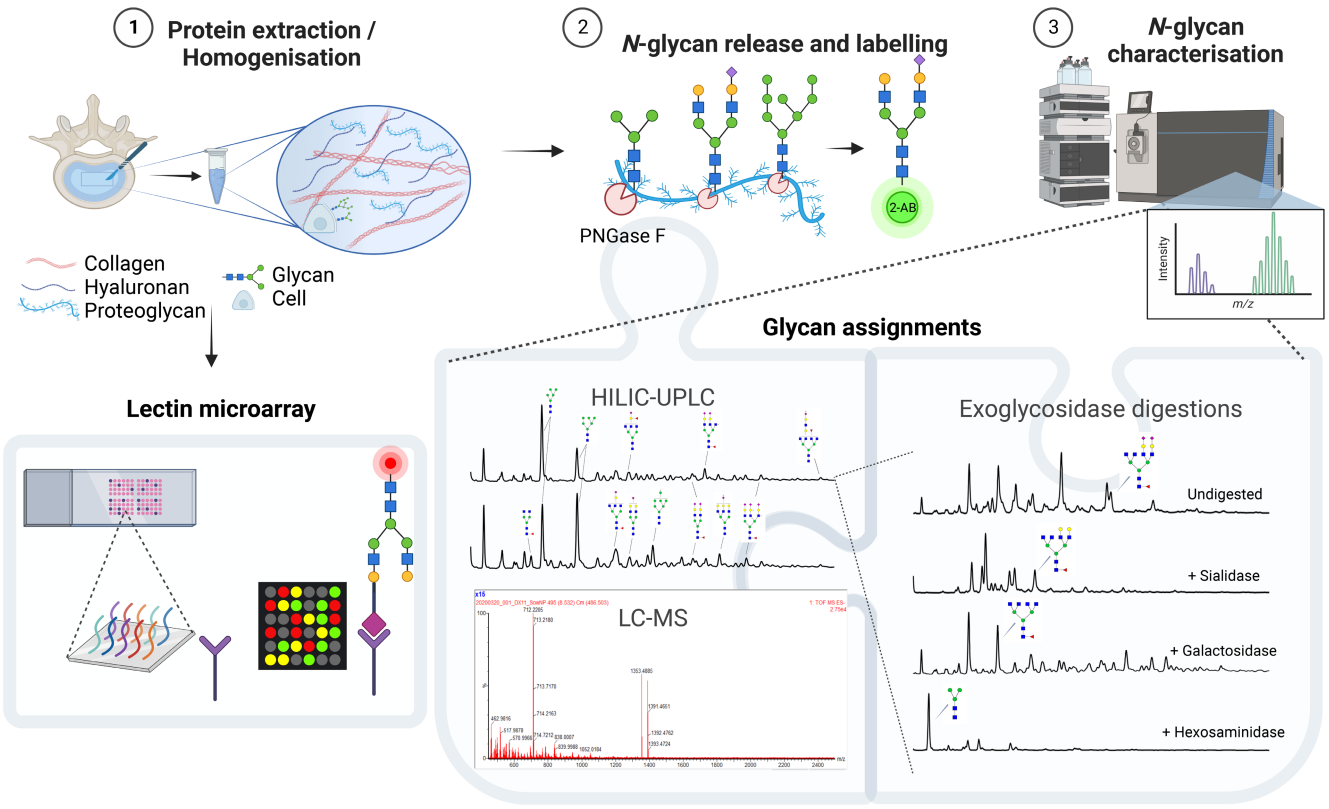

FIGURE 1 Schematic of the methodical approach to characterize the *N*-glycome from nucleus pulposus tissue derived from pigs. (1) Glycoproteins were extracted from the tissue through homogenization and either used in lectin microarray or further processed, (2) *N*-glycans were enzymatically released and labeled, and (3) characterized using UPLC, mass spectrometry. Created with BioRender.com.

glycoproteins was collected following centrifugation at 16,000*g* for 20 min at 4°C and vacuum dried (Savant™ SPD131DDA SpeedVac™ Concentrator, Fisher, Ireland) for subsequent lectin microarray, and also for *N*-glycan release for liquid chromatography and mass spectrometry measurements. Briefly, SDS gels were formed around dried homogenate to immobilize and prevent loss of the samples, reduced and alkylated by DTT and IAA, respectively, and then washed with acetonitrile in 2 mL round bottom tubes as described previously.[25] *N*-linked glycans were cleaved by PNGase F, eluted, and labeled with 2-AB. Samples were incubated with 2-AB at 65°C for 2 h and the excess was cleaned by glass fiber plates using 3MM Whatman® paper;the last elution of the labeled glycans was done with water followed by a final vacuum dry.

2.4 | Exoglycosidase digestions

To remove target monosaccharides, 2-AB labeled *N*-glycans were digested with a series of exoglycosidases listed in Table S1. 2AB-labeled glycans were digested in a volume of 10 µL for 18 h at 37°C in 50 mM sodium acetate buffer, pH 5.5 (except in the case of α1,2/3/6 Mannosidase where the buffer was 50 mM sodium acetate, 2 mM Zn^{2+}, pH 5.0). Enzymes were deactivated at 65°C for 15 min and then cleaned up using a 10 kDa MWCO microcentrifuge filtration tube (Pall, 516-8491).

2.5 | HILIC/WAX UPLC and mass spectrometry

Hydrophilic interaction ultra-performance liquid chromatography (HILIC-UPLC) allows glycans to be separated according to their hydrophilicity and sizes as the smaller glycans elute faster than larger ones. The runs are performed using Acquity glycan BEH amide 1.7 µm particles in a 2.1 × 150 mm column (Waters, USA) on H class Acquity UPLC (Waters, USA). The column temperature was kept at 40°C using a Waters temperature control module. Samples were suspended for injection in 70% acetonitrile and run for 30 min in a method consisting of solvents of 50 mM ammonium formate at pH 4.4, and acetonitrile as previously described.[21,26] Fluorescence detection is done at Ex/Em: 320/420 nm using a Waters Acquity fluorescence detector. To calibrate the system and prevent handling errors, a dextran ladder is used as standard and later analyzed to generate glucose units (GUs).[27]

DMB assay and weak anion exchange (WAX)-UPLC were performed to determine the type of sialic acids and the level of sialylation. Sialic acids from undigested *N*-glycans were released and then labeled with 1,2-diamino4, 5-methylenedioxybenzene (DMB) (Ludger Ltd.) according to the manufacturer's protocol[28] for detection in WAX-UPLC. Samples were run using an Acquity UPLC separations module (Waters, USA) equipped with a fluorescence detector (Waters, USA) controlled by an Empower Chromatography Workstation. The analytical column used is a LudgerSep-uR2, with 2.1 × 50 mm, 1.9 µm particle size. Mobile phase solvents consist of acetonitrile:methanol:water 9:7:84 (solvent A) and acetonitrile (solvent B). The column temperature is kept at 30°C during the 15 min run, and fluorescence is detected at Ex/Em: 373/448 nm.

For detection of charged glycans, a DEAE (di-ethyl-amino-ethyl) anion exchange column 75 × 7.5 mm, 10 µm particle size (Waters, USA) was used. 20% v/v acetonitrile in water (solvent A) and 0.1 M ammonium acetate buffer pH 7.0 in 20% v/v acetonitrile (solvent B) was used in a 30 min long method.

Liquid chromatography-mass spectrometry (LC-MS) was performed in a Waters Xevo G2 QTof mass spectrometer in negative mode with ACQUITY UPLC (Waters, USA, 1 ppm resolution) and BEH Glycan column (1.0 × 150 mm, 1.7 µm particle size). *N*-glycans were eluted in a 60°C column at a flow rate of 150 µL/ min over 30 min run using buffer A (50 mM ammonium formate, prepared with 50 mM formic acid, adjusted to pH 4.4 with ammonium hydroxide solution) and buffer B (ACN).[26,29] Fluorescence is detected at Ex/Em: 330/420 nm as a part of liquid chromatography. Data collection and analysis were performed using MassLynx software (v4.1, Waters).

2.6 | Lectin microarray

Lectin binding profiles were obtained by Asparia Glycomics (San Sebastián, Spain), using well-based microarray slides containing a selection of different lectin spots. A complete list of lectins used in the study is given in Table S2. Briefly, glycoproteins extracted by mechanical homogenization method as explained in above in section 5.3 at a concentration of 100 µg/mL were labeled with Alexa Fluor™ 647 NHS ester and incubated on duplicate microarray slides, fabricated using lectin solutions at 0.4–0.5 mg/mL, for 3 h at room temperature. Slides were then washed for 5 min with phosphate buffer saline and scanned with a G265BA microarray scanner (Agilent Technologies). To quantify the relative fluorescence intensities, images were analyzed using Pro Scan Array Express software (PerkinElmer).

2.7 | Reproducibility and data analysis

For this study, all tissue samples from each age group were pooled and then processed and analyzed and therefore

we had no replicates for reproducibility. UPLC-MS data should thus be considered descriptive. However, our method is based on previously optimized reproducible protocols with an established coefficient of variance.[30]

Chromatograms from the pooled samples were separated into 67 glycan peaks (GPs) in the young and 76 peaks in the mature NP for analysis and integrated to enable calculation of the abundance of *N*-glycans based on the area of the peaks. In this manuscript, GPs are simplified to a total of 27 to unify both profiles and draw attention to the high-abundance glycans. Based on the digestion profiles, we have assigned suggested glycan structures and abundances to the main profile. The expected mass of the glycan is then identified in the mass spectrometry data using MassLynx software. Glycan structures were accepted as present if the error was <20 parts per million between expected and theoretical mass which was calculated using GlycoWorkbench 2 software.[31]

Lectin microarray was performed in two technical replicates using the pooled samples from the two age-groups. Data were analyzed by multiple t tests using the Holm-Sidak method for multiple comparisons ($\alpha = 0.05$) and performed using GraphPad Prism software.

3 | RESULTS

3.1 | Notochordal cell-rich nucleus pulposus has a distinct *N*-glycome profile

A general outlook of the *N*-glycome of young and mature porcine NP was obtained by hydrophilic interaction ultra-performance liquid chromatography (HILIC-UPLC) before *N*-glycans were identified and glycosylation traits summarized. The approach for structural assignments of glycans using a series of exoglycosidase digestions in combination with mass spectrometry is outlined in Figure 1. The analysis of HILIC-UPLC of the digested samples can be found in Table S3 and the confirmation of glycans based on liquid chromatography-mass spectrometry (LC-MS) can be followed in Table S4. *N*-glycome profiles interpreted from the chromatograms were similar, but not superimposable, indicating age-related differences (Figure 2).

We have assigned a total of 317 structures to the young NP, and 384 to the mature NP, including isomers. The most abundant *N*-glycans in both profiles are compared in Table 1. Based on the structure assignments to the peaks, *N*-glycans were summarized according to their content of galactose, antenna, fucose, sialic acid, and other modifications (Figure 3, Table 2). In both samples, two of the highest peaks belonged to oligomannose species. Mainly, M5 (GP6) and M6 (GP9) were the most abundant *N*-glycans, followed by M7 (GP12) and M8 (GP16) in the young NP (Figure 3A).

Antennary structures were found to be one of the predominant compositions in both age groups. Biantennary *N*-glycans were the most abundant among mono- to tetraantennary structures, with similar abundances totalling 73.4% and 76.6% in young and mature NP, respectively (Figure 3B).

Core fucosylation was one of the highest motifs in both samples with approximately 45% abundancy in both age groups. Total fucosylation in the younger NP was lower than that in the mature NP; this difference comes from 1.3% outer arm fucosylation in the young as opposed to 6.5% in the mature NP (Figure 3C).

Galactosylation was found to be 61.8% of total *N*-glycans in young and 65.0% in mature NP, including with and without sialylation. Tri- and tetragalactosylated structures were more abundant and mono- and digalactosylated structures were less abundant in the younger NP than in the mature NP (Figure 3D).

3.2 | Sialylation dominates *N*-glycans with higher α(2,3) link in young notochordal cell-rich nucleus pulposus

Sialylation also had one of the highest relative abundances with 46.8% of total *N*-glycans in young and 50.5% in mature NP. Mono- and disialylated glycans also had a slightly higher abundance in the mature NP; tri- and tetrasialylation were lower in general but higher in the young NP (Figure 3E). Some of the most striking differences, however, were found in the sialic acid linkages. α(2,6)-linked sialic acid was the main linkage type for both samples comprising 25–31% of all sialylation, higher in mature NP (Figure 3F). In contrast, α(2,3)-linked sialic acid was higher in the younger NP (14.4%) than in the older with only 5.3%. The instances of α(2,3/6), polysialic, or sialic acid with unknown linkages were 14.5% in the mature and 7.1% in the young NP. The dominant sialic acid type was 5-*N*-acetylneuraminic acid (Neu5Ac), with5-*N*-glycolylneuraminic acid (Neu5Gc) comprising <2%. This was also confirmed by 1,2-diamino-4,5-methylenedioxybenzene (DMB) assay and weak anion exchange chromatography (WAX) where the undigested *N*-glycans were separated by charge. Interestingly, integration of peaks in WAX chromatograms indicated 30% and 43% sialylation in young and mature NP, respectively (Figure 4), lower than what is assigned via exoglycosidase digestions and LC–MS. However, the peak for 2-aminobenzamide (2-AB) label and the contaminant peak, also overlap with the nonsialylated S0 fraction; therefore, the sialylation is underestimated in this method. When comparing the ratios of charged peaks on WAX and HILIC-UPLC, higher levels

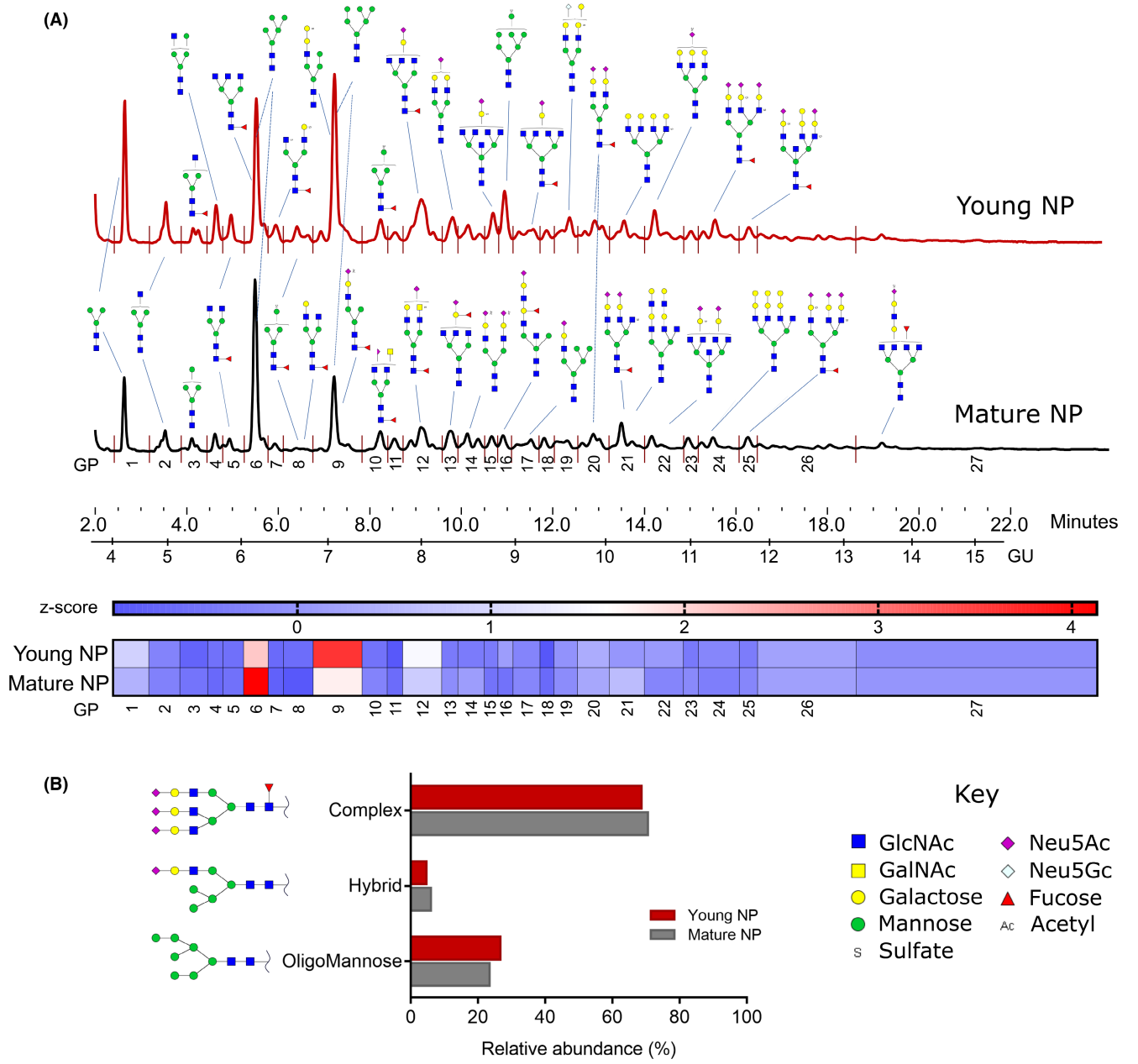

FIGURE 2 General outlook of the *N*-glycome of young and mature nucleus pulposus (NP) derived from notochordal cell-rich porcine intervertebral discs. Representative HILIC-UPLC chromatograms of *N*-glycome from young and mature NP. Some of the most abundant glycans are shown relative to their peak shown with the changes in glycan peaks (GPs) based on their *z*-score. (B) Three major groups of glycans and their relative abundance to total glycans (left), the key to monosaccharide representations (right). GlcNAc: *N*-acetylglucosamine, GalNAc: *N*-acetylgalactosamine, Neu5Ac: 5-*N*-acetylneuraminic acid, Neu5Gc: 5-*N*-glycolylneuraminic acid.

of tri- and tetrasialylated glycans (especially in mature NP), and lower mono- and disialylated glycans were present in WAX than those in HILIC-UPLC data. This could be because the WAX separates not only according to the number of sialic acids, but also due to other charges, such as sulfation and acetylation, which move the particular glycans into the higher charged peaks.

Sulfation was one of the most commonly observed modifications, decorating galactoses and *N*-acetylglucosamines (GlcNAcs) with 20.2% in young and 21.7% in the mature NP. We also found acetylated glycans in our analysis in a slightly higher abundance in the mature NP than in the younger: 4.3% and 1.8%, respectively (Figure 3G). This is accompanied by more abundant α-linked galactose-containing glycans in the younger NP (19.7%) than those in the mature (5.3%), and a slightly lower number of poly-*N*-acetyllactosamine structures in the younger NP (9.4%) than that in the mature (12.2%).

TABLE 1 The most abundant N-glycans in each glycan peak in young and mature nucleus pulposus (NP) derived from pigs.

	Young NP			Mature NP		
GP	Glycan name	Peak area (%)	GU	Glycan name	Peak area (%)	GU
1	M3	6.15	4.13	M3	5.00	4.11
2	A1	2.88	4.83	A1	2.69	4.75
3	FA1	1.61	5.26	M4	2.06	5.12
4	M4A1	2.17	5.60	A1G1(s)1 & A1(s)1G1	1.56	5.56
5	FA2	2.11	5.81	FA2	1.92	5.68
6	M5	9.57	6.14	M5	16.65	6.10
7	FA2(s)1G1(s)1	1.85	6.38	M4A1G1(s)1	1.15	6.46
8	FM5	2.00	6.63	FA2G(4)1	0.76	6.60
9	M6	13.61	7.04	M6	9.19	7.02
10	FM6	2.22	7.52	FA2GalNAc1S(6)1	2.79	7.40
11	FM4A1G1(s)1S(3)1	1.12	7.67	M7	1.71	7.64
12	M7	7.82	7.93	FA2G1GalNAc(s)1S(6)1	6.24	8.03
13	A2G(4)2S(6)1	2.53	8.25	A3F(2)1G1S(6)1	3.26	8.22
14	FA4G1GlcNAc1	2.55	8.40	A2G2S(Ac)2	4.03	8.50
15	A4BG1(s)1S(6)1	2.56	8.66	A2F(2)1G2(s)1S(6)1	2.01	8.65
16	M8	3.98	8.78	A1BF(2)1G1Lac1S(6)1	1.98	8.77
17	FA4G(4)1S(6)1	2.93	9.06	FM5A1G(4)1S(6)1	2.95	9.07
18	FA2GalNAc2S(6)2	1.09	9.24	A4G(4)2GalNAc2	1.58	9.22
19	A2G(s)1G(3)1Gal1Sg(3)1 A2G2F1S(Ac)2	3.51	9.50	A3BGalNAc2S(6)2	3.20	9.48
20	FA2G2S(6)2	4.61	9.79	FA2G2S(6)2	4.47	9.78
21	FA2G2Gal2S(3)1	3.70	10.14	FA3(s)1G(4)2S(3,6)2	5.51	10.11
22	A2BG2Lac1Gal2	3.86	10.51	FA4BG2(s)1S(3,6)2	2.90	10.59
23	A2F1G2Lac2S(6)1	2.47	11.11	FA4G(4)2S(6)2	3.08	11.10
24	FA2(s)1G2(s)1Gal1S(3,6,8)3	3.01	11.26	A4G(4)3Gal3 FA2G(2)Gal2S(6)2	2.55	11.43
25	FA3B(s)1G3(s)1Gal1S(3,6)2	2.61	11.69	FA3(s)1G3(s)1S(3,6,6)3	2.91	11.68
26	A4BG4(s)1S(6)3	4.18	12.96	A4G4Lac1S(3)2	4.18	12.71
27	A3G3GlcNAc1Lac2Gal2S(3)2	3.31	14.11	A4F1G2Lac2S(3)2	3.65	13.40

Note: Most abundant glycans of the same glycan peak in both samples are highlighted in gray.

Abbreviations: All N-glycans have two core GlcNAcs; F at the start of the abbreviation indicates a core-fucose α1,6-linked to the inner GlcNAc; Mx, number (x) of mannose on core GlcNAcs; Ax, number of antenna (GlcNAc) on trimannosyl core; A2, biantennary with both GlcNAcs as β1,2-linked; A3, triantennary with a GlcNAc linked β1,2 to both mannose and the third GlcNAc linked β1,4 to the α1,3-linked mannose; A4, GlcNAcs linked as A3 with additional GlcNAc β1,6 linked to α1,6 mannose; B, bisecting GlcNAc linked β1,4 to β1,4 mannose; Gx, number (x) of β1,4 linked galactose on antenna; Galx, number (x) of galactose α1,3 linked to galactose; F(x), number (x) of fucose linked α1,2/3 to antenna GlcNAc; Sx, number (x) of Neu5Ac sialic acids linked to galactose; Sgx, number (x) of Neu5Gc sialic acids linked to galactose; Lac(x), number (x) of lactosamine (Galβ1-4GlcNAc) extensions; s and Ac are sulfated and acetylated glycans, respectively. Numbers in brackets indicate monosaccharide linkages. If the monosaccharide has no label, it is linked by an unknown linkage.

3.3 | Total glycosylation by lectin microarray confirms high sialylation and fucosylation

Glycosylation profiles were also determined by lectin microarray which, in contrast to the findings shared so far, targets not only *N*-glycans but other glycan types too (Figure 5). This approach gives an idea about the abundance of the *N*-glycans relative to total glycans as the differences between the LC-MS assignments and the lectin microarray must be due to the presence of other type of glycans such as *O*-glycans. Most strikingly, fluorescence from DSL and STL was the strongest for both samples indicating multi antennary *N*-glycans and was significantly higher for the mature NP. A high level of α(2,6)-linked sialylation was also indicated by the strong SNA but weak (α-2,3 specific) MAL-I

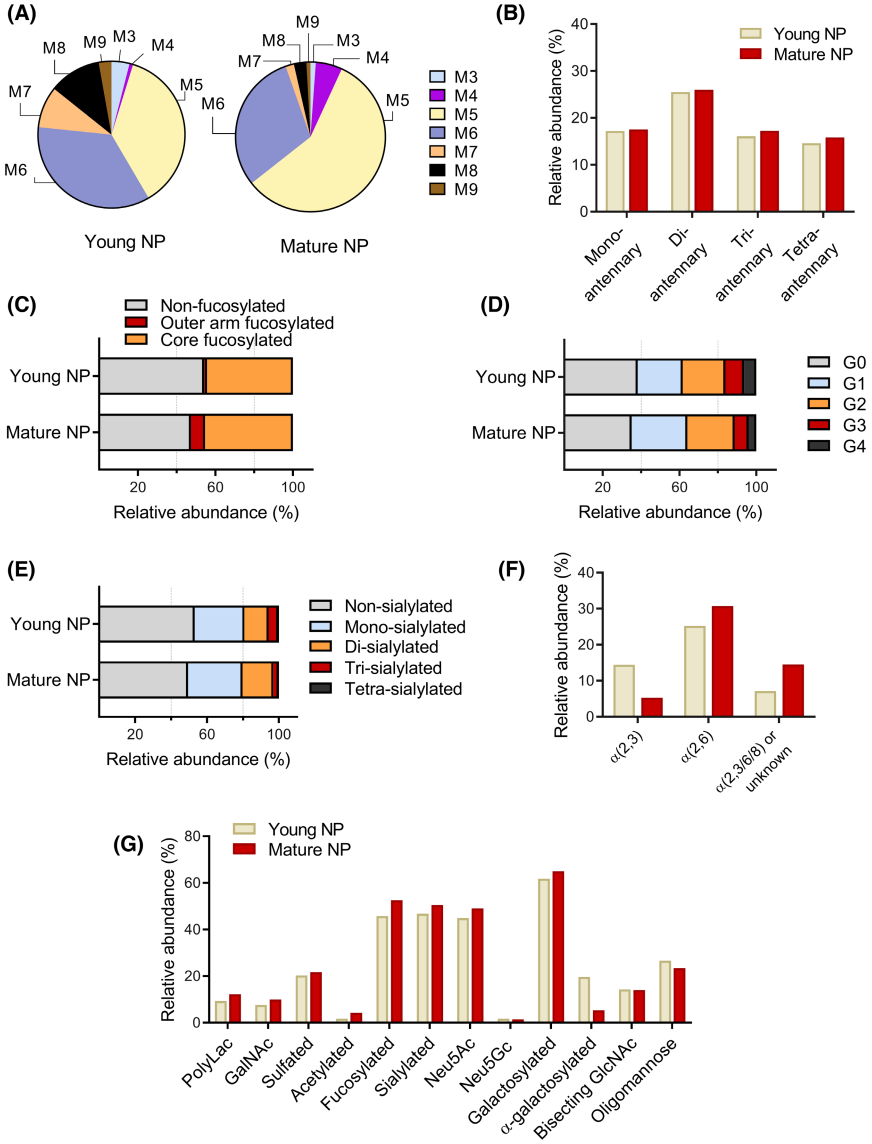

FIGURE 3 Relative abundances of major *N*-glycan features in notochordal cell-rich young and mature porcine NP. Classification of and relative abundance to total *N*-glycans based on their (A) mannose content given as a percentage to total mannosylation, (B) antennary distribution, (C) degree of fucosylation, (D) galactosylation, (E) degree of sialylation, (F) the type of sialic acid linkage, and (G) other features of interest where each feature is presented as a percentage to total *N*-glycans. Raw data and analysis are given in Tables S3 and S4. PolyLac: poly-*N*-acetyllactosamine, GalNAc: *N*-acetylgalactosamine, Neu5Ac: 5-*N*-acetylneuraminic acid, Neu5Gc: 5-*N*-glycolylneuraminic acid, GlcNAc: *N*-acetylglucosamine.

binding in comparison. While we assigned higher α(2,3) sialylation via HILIC-UPLC analysis of *N*-glycans, this must be undetected in the lectin array where larger glycan species are present. NPL and GNA binding revealed oligomannose and hybrid type glycans. Fucose-binding lectins also presented high intensity, especially for AAL and AAA. This was also supported by PSA binding, which has an increased affinity to mannose in the presence of α(1,6) fucose.[32] Strong binding to RCA lectin, which interacts with galactose and GalNAc, together with weak binding to HAL, a GalNAc lectin, suggests a high level of galactosylation but limited terminal GalNAc.

Overall analysis indicated a high level of antennary structures, galactosylation, α(1,6) fucosylation, mannosylation, and α(2,6) sialylation (Figure 4B), which are consistent with our findings in chromatography and spectrometry-based manual assignments.

4 | DISCUSSION

In this study, we aimed to characterize the *N*-glycome of notochordal cell (NC)-rich nucleus pulposus (NP) from young and mature pigs in the context of healthy but aging discs. To be able to assess the effect of maturation without the confounding factor of NC loss, we chose to use a species with NC-rich IVDs. Unlike humans, mature pigs maintain their NCs beyond puberty and so are a good model for the study of the aging effects on NC maturation.[33] This is not possible in humans; in human IVDs, the vacuolated NCs are already lost in childhood and any collection of such scarce tissues comes with ethical concerns. We used an exoglycosidase panel in UPLC in tandem with mass spectroscopy to assign proposed *N*-glycan structures to the chromatogram peaks by determining specific linkages and monosaccharide configurations. As

TABLE 2 Summary of N-glycan traits in young and mature nucleus pulposus (NP) rich in notochordal cells according to their relative abundances in UPLC chromatograms. Each secondary trait is given as relative abundance to total N-glycans.

Trait	Relative abundance (%)	
	Young	Mature
Oligomannosidic	26.6	23.4
M3	1.1	0.3
M4	0.2	1.3
M5	9.8	13.5
M6	9.3	7.1
M7	2.4	0.4
M8	3.1	0.6
M9	0.7	0.2
Hybrid	4.7	6.0
Complex	68.7	70.6
Non-fucosylated	54.2	47.3
Fucosylated	45.8	52.7
Core fucosylated	44.3	45.4
Outer arm fucosylated	1.5	7.3
Non-sialylated	53.2	49.5
Sialylated (S1–S4)	46.8	50.5
Monosialylated (S1)	27.6	30.2
Disialylated (S2)	13.5	17.2
Trisialylated (S3)	5.4	3.0
Tetrasialylated (S4)	0.4	0.1
α(2,3) only	14.4	5.3
α(2,6) only	25.2	30.7
α(2,3/6/8) or unknown	7.1	14.5
Neu5Ac (S)	45.0	49.1
Neu5Gc (Sg)	1.8	1.4
Non-galactosylated	38.2	35.0
Galactosylated (G1-G4)	61.8	65.0
Monogalactosylated (G1)	23.4	29.0
Digalactosylated (G2)	22.2	24.7
Trigalactosylated (G3)	9.7	7.3
Tetragalactosylated (G4)	6.4	4.0
Non-antennary	26.6	23.4
Antennary	73.4	76.6
Monoantennary	17.2	17.6
Biantennary	25.5	26.0
Triantennary	16.1	17.2
Tetraantennary	14.6	15.8
Secondary traits		
Polylac	9.4	12.2
GalNAc	7.6	10.0
Sulfated	20.2	21.7
Acetylated	1.8	4.2
α-Galactosylated	19.7	5.3
Bisecting GlcNAc	14.3	14.0

Abbreviations: GalNAc, N-acetylgalactosamine; GlcNAc, N-acetylglucosamine; Neu5Ac, 5-N-acetylneuraminic acid; Neu5Gc, 5-N-glycolylneuraminic acid; polylac, poly-N-acetyllactosamine.

exoglycosidases remove certain monosaccharide types one at a time, it enables reconstruction of a glycan structure from a most digested state, and also help to separate glycans which MS cannot (such as linkage isomers). This combined approach allows the assignment of glycan structures that is more precise than one using only histochemical or spectrometric analysis. We found the general profile of young and mature NC-rich NPs to be similar, a profile which therefore could be used for species comparisons of the NP in further studies. However, there were striking differences in outer arm fucosylation, abundance in certain oligomannosidic *N*-glycans and α(2,3)-linked sialic acid, which can be attributed to aging.

Our findings suggest that the outer arm fucosylation may be involved in aging of the disc, a process that is characterized by high catabolic activity leading to the degradation of the ECM proteins.[34,35] There are very few publications regarding the bioactivity of outer arm fucose aside from the ABO blood group antigens. However, a particularly interesting study found that the removal of outer arm fucose increases the inhibitory effect of the tissue inhibitor of metalloproteinases 1 (TIMP1) on matrix metalloproteinase 3 (MMP3), suggesting that α(1,3)-linked outer arm fucose is involved in the activity of MMP3 which has a proteolytic activity on the ECM.[36] This also aligns with the increased matrix remodeling seen in NC transition to chondrocyte-like cells involving canonical Wnt signaling, a process associated with NP aging and degeneration.[37]

High levels of core fucosylation were maintained in healthy NC-rich NP tissue during maturation which was an unexpected finding considering that core fucosylation is arguably affected with aging.[38,39] Core fucosylation is involved in conditions such as cancer,[40–42] cardiac regenerative capacity,[43] liver disease,[44] and autoimmune diseases,[45] potentially through disruption of cell recognition, signaling, and adhesion.[46,47] Core fucosylation by α1,6-fucosyltransferase is also crucial for development as shown by the lethality rate and growth retardation accompanying dysregulation of TGFβ-1 signaling in α1,6-fucosyltransferase knockout model in mice.[22] In the present study, core fucosylation is understood to be a

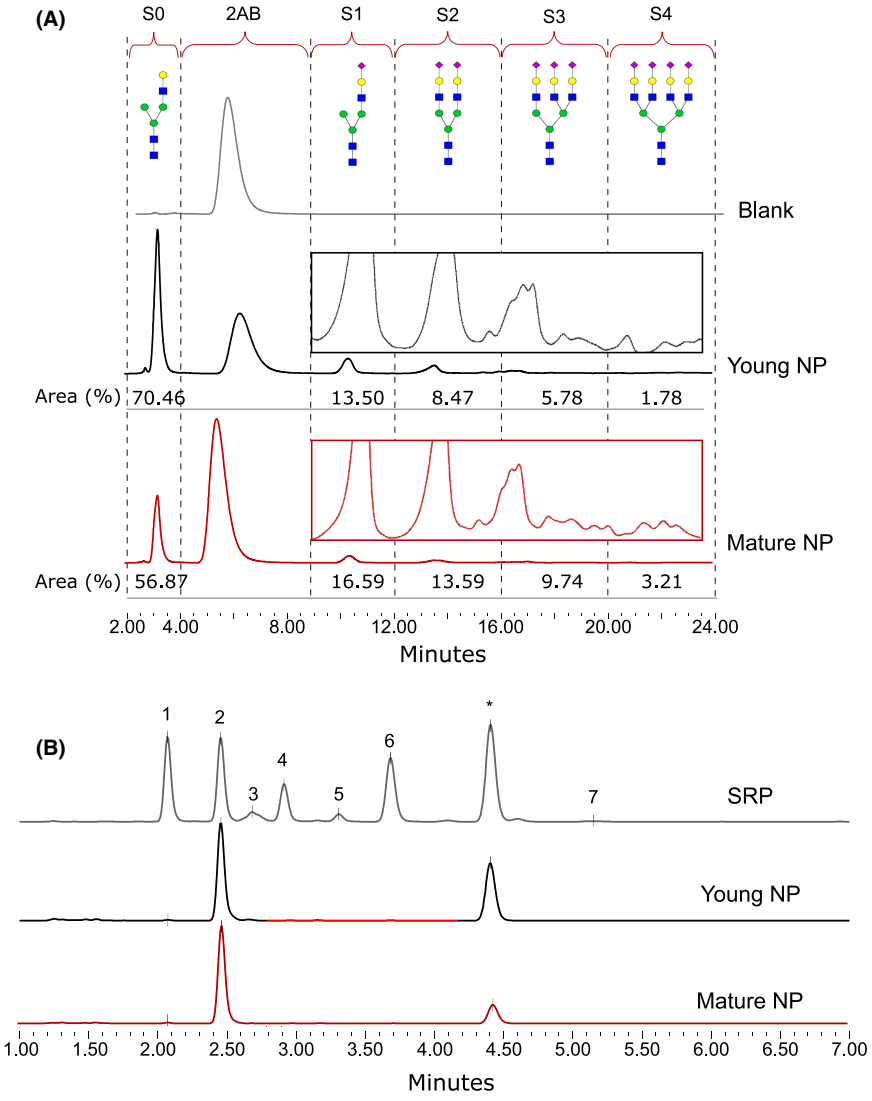

FIGURE 4 Summary of sialylation in young and mature NP. (A) Charged N-glycans attributed to the number of sialic acids, in fractions from nonsialylated (S0) to tetrasialylated (S4), and (B) the type of sialylation found the young and mature NP in reference to the sialic acid reference panel (SRP) where 1 = Neu5Gc; 2 = Neu5Ac; 3 = Neu5,7Ac2; 4 = Neu5Gc,9Ac; 5 = Neu5,8Ac2; 6 = Neu5,9Ac2; 7 = Neu5,x,xAc3 (where × is an unknown acetyl position); * = Reagent.

characteristic of the NC-rich healthy NP studied. It seems not to be age-dependent in growing pigs up to young adults and as such may strongly relate to the maintenance of NCs. Establishing an actual function of core fucosylation does not seem practicable as it is thought to be affected by the availability and the structure of the *N*-glycan rather than by the peptide sequence the glycan is built on.[48]

O-Acetylation of sialic acids on *N*-glycans is relatively common in aging NC-rich NP. At non-reducing termini of glycan chains, sialic acids are found in a position to cap the glycans to either inhibit or allow molecular interaction and in particular in the role of a receptor in recognition. The alterations in the sialic acid levels can be interpreted as a change in the cellular activity as a result of a disturbance in the homeostasis, such as inflammation. In addition, *O*-acetylation of the sialic acids is mostly associated with cancer and immune response.[49,50] For example, it is suggested that acetylated Neu5Ac contributes to immune cell-mediated cytotoxicity.[51] However, it does not seem critical to our perspective in this study as the nucleus pulposus is somewhat isolated from the immune response under normal conditions. This leads us to speculate that acetylation may indicate processes involved in aging of NP.

Notably, α-linked galactose (α-gal) containing glycans occurred more in the younger NP. This is not the first report of α-gal presence in a younger tissue; it was noted as well in neonatal porcine islets[52] and murine cardiac tissue.[53] On the other hand, we also noted that some α-galactosylated *N*-glycans on immunoglobulin G3, namely, FA2G2Gal1 and FA2G2Gal1S1 increased with age in mice.[54] Yet, we did not pursue any consequent implications further because, α-gal is mainly associated with the immunoglobulin E antibody reaction (known as red meat allergy) and issues around xenotransplantation[55,56] and is beyond the scope of this manuscript. The relevance of α-gal, and any other specific glycan that contains it, to aging, inflammation, or species remains to be seen.

Notwithstanding the relatively low number of publications relating to glycosylation of the IVD, a recent study of the changes in the glycosylation in degenerative

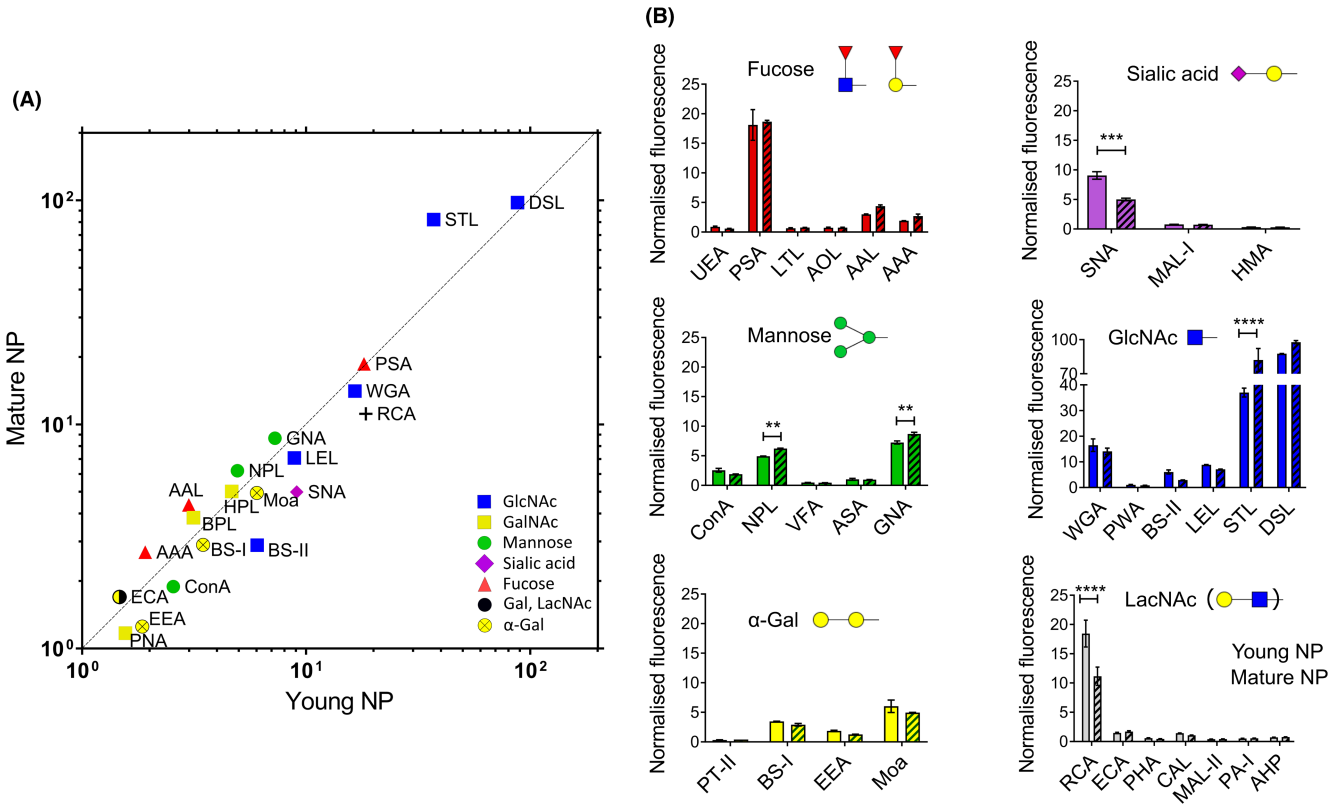

FIGURE 5 Lectin binding profile in young and mature nucleus pulposus (NP). (A) Scatter plot of lectins with highest fluorescence intensities and (B) lectin binding profiles based on main glycosylation motifs. Data are collected from glycoproteins of two technical replicates of pooled biological replicates, analyzed with multiple *t* test using the Holm-Sidak method, $\alpha = 0.05$, $^{**}p < 0.0021$, $^{**}p < 0.0002$, $^{****}p < 0.0001$, and represented by mean ± SEM. A complete list of the lectins and their specificities is given in Table S2, and readily indicated in the panel. GlcNAc, *N*-acetylglucosamine; GalNAc, *N*-acetylgalactosamine; Gal, galactose; LacNAc, *N*-acetyllactosamine.

NP reported hyper sialylation and core fucosylation in a cytokine-mediated inflammation model.[57] However, the effect of aging may have been obscured by comparing degenerative mature NP with healthy young NP, with the assumption that the glycosylation patterns of interest in mature discs are universal. While the low level of mannosylation and α(2,3)-linked sialic acid in inflammation is in line with our findings, existing variations such as lower outer arm fucosylation and higher α(2,6)-linked sialic acid suggest that maturation does not involve processes identical with those of degeneration of the NP. Furthermore, the addition of *O*-linked β-*N*-acetylglucosamine was found to be directly proportional to the degeneration level of the disc.[58] This is thought to be related to the stress induced uptake of glucose by the resident cells. In findings that are the opposite of ours, α(2,6)-linked sialic acid is reported to be higher in the young bovine NP; however, a lack of observed vacuolated NC was pointed out in this study,[59] suggesting perhaps that it is the specific α(2,3) linkage which has a capacity to maintain the NC glycosylation phenotype.

Aging and the onset of IVD degeneration seem to be creating a paradox in terms of the disappearance of the NCs. The notochord is the developmental origin of the NP and hypothesized to be correlated with the maintenance of a healthy phenotype in the disc.[33,60] In an effort to eliminate one unknown in this equation, we focused on the changes in *N*-glycosylation in aging by using porcine tissue as the pig is one of the species that do not lose their NC population upon maturity, which is the case with humans. Assuming that many of the protein functions and interactions are governed by glycosylation, the NC-niche must have a distinct *N*-glycome too. For instance, tail regeneration in zebrafish, which is essentially orchestrated by NCs, has been shown to be inhibited by the interfering with GlcNAc incorporation to the *N*-glycan core.[61] *N*-linked glycosylation by uridine diphosphate *N*-acetylglucosamine (UDP-GlcNAc) is enabled by a glucose flux through the hexosamine biosynthetic pathway. Interestingly, this pathway also provides a substrate to the synthesis of the hyaluronic acid, one of the main components of the NP contributing to its GAG-rich niche. In addition, our findings of high levels of similar antennary structures comprising over 70% of all glycans taken together with the notable presence of GlcNAc containing glycans indicated by strong binding of STL, WGA,

and LEL lectins encourage the idea that the addition of GlcNAc to the main core is crucial for the regenerative capabilities through matrix production of NCs.

Aging of the *N*-glycome has already been demonstrated in the context of cells and tissues. A higher abundance of sialylated and polysialylated glycans (along with an increase in the expression of their corresponding sialyltransferases, St3gal2 and St6gal1), and a lower expression especially of M6 oligomannosidic types are correlated with aging in the murine epidermal stem cells and cardiac tissue, respectively.[53,62] However, also in a murine model, decreased sialylation and increased mannosylation in aging are shown[38] indicating the complexity of *N*-glycome not only in IVD, but also other biological systems.

The strong impact of glycosylation toward the enzyme function and disease progression has been demonstrated through NC markers.[5,63] It is tempting to hypothesize that NC markers are highly mannosylated and hence biologically more active. For example, the biologic activity of CD24 in cancer progression, also a proposed NC marker, is shown to dampen with low expression of the MAN1A1 enzyme responsible for M5 production at the beginning of *N*-glycan synthesis.[64] The presence of NCs may be one of the many factors accounting for the high abundance of oligomannosidic *N*-glycans in our analysis. It is possible that the abundance of M5 is a result of increased *N*-glycan synthesis and not the end product. A study of glycosyltransferase expression such as *N*-acetylglucosaminyltransferase I or *N*-glycan characterization in endoplasmic reticulum and Golgi may determine the correct answer to that question.

Certain limitations to this study should be noted. First, reproducibility could not be achieved and statistical analysis could not be performed as all the biological samples are pooled. However, the study is based on the previous studies where a coefficient of variation is calculated and a robust protocol established. We show differences in pooled samples rather than individual samples, therefore we have no coefficient of variation in individual animals, but we have indicated major differences in depth in pooled samples. Second, glycan assignments based on exoglycosidase digestions and mass spectrometry are not automated, and therefore are open to interpretation by each analyst. Even so, without the extensive work required for this manual analysis, such features as linkage information would not be captured using only generic methods such as lectin binding or immunohistochemistry. Third, the IVDs were not graded for degeneration prior to the sampling process. However, adjacent lumbar IVDs of the porcine donors had normal macroscopic appearance. In view of results presented here, this study provides observations which enhance our understanding of glycosylation's importance in IVD degeneration and in designing glyco-therapeutics for it.

5 | CONCLUDING REMARKS

Glycosylation is key to understanding disease progression, glycan function, and protein activity. The dynamic and complex nature of glycosylation drives many researchers to question limited aspects of it such as only *N*-glycans. Certain glycosylation patterns are occasionally reported to be altered in a contradictory way; this makes it hard to identify and assign specific features to glyco-modifications. Nonetheless, studies show differences between diseased and healthy glycome that are sometimes significant. Here, we showed changing glycosylation patterns in aging NP, and also identified numerous individual *N*-glycans. We have elucidated motifs through identification of *N*-glycans and have a view of the *N*-glycome in the NP that is global rather than one which considers just the specific functions of *N*-glycans. For such a condition as intervertebral disc degeneration that accompanies aging, we believe our study illustrates specifically the effect of aging in the context of the *N*-glycome of the nucleus pulposus.

AUTHOR CONTRIBUTIONS

BG, AP, and RS conceptualized the project and designed the experiments. BG conducted experiments, analyzed all data, and drafted the manuscript; EM acquired mass spectrometry data; JM performed sialic acid detection experiments; MAT procured the spinal segments and provided critical assessment of the manuscript; AP and RS supervised the project and interpreted the results.

ACKNOWLEDGMENTS

This project has received funding from the European Region Development Fund and Science Foundation Ireland (SFI) under Ireland's European Structural and Investment Fund under grant number 13/RC/2073_P2, and the European Union's Horizon 2020 research and innovation program under grant agreement No 825925 as a part of the iPSpine project. MAT is financially supported by the Dutch Arthritis Society (LLP22). The authors would like to thank Hayden Wilkinson from NIBRT for support with the methodology; thanks also to Lisanne Laagland, Dr. Frances Bach, and Adel Medzikovic from Utrecht University for providing spinal segments; and the late Mr. Anthony Sloan for editorial assistance. Open access funding provided by IReL.

CONFLICT OF INTEREST STATEMENT

The authors of this manuscript declare no conflict of interest.

DATA AVAILABILITY STATEMENT

The mass spectrometry raw data of undigested N-glycans and assigned structures are available in GlycoPOST at https://glycopost.glycosmos.org/preview/38954402063d3c299bc7bc (PIN: 5455) under project ID: GPST000318. UPLC chromatograms are given in the article and the raw peak area data are provided in Table S3.

ORCID

Abhay Pandit https://orcid.org/0000-0002-6292-4933

REFERENCES

1. Freemont AJ. The cellular pathobiology of the degenerate intervertebral disc and discogenic back pain. *Rheumatology*. 2008;48(1):5-10.
2. Lawson L, Harfe BD. Notochord to nucleus pulposus transition. *Curr Osteoporos Rep*. 2015;13(5):336-341.
3. Cappello R, Bird JL, Pfeiffer D, Bayliss MT, Dudhia J. Notochordal cell produce and assemble extracellular matrix in a distinct manner, which may be responsible for the maintenance of healthy nucleus pulposus. *Spine*. 2006;31(8):873-882.
4. Götz W, Osmers R, Herken R. Localisation of extracellular matrix components in the embryonic human notochord and axial mesenchyme. *J Anat*. 1995;186(Pt 1):111-121.
5. Rodrigues-Pinto R, Ward L, Humphreys M, et al. Human notochordal cell transcriptome unveils potential regulators of cell function in the developing intervertebral disc. *Sci Rep*. 2018;8(1):12866.
6. Wang Y, Bai B, Hu Y, et al. Hydrostatic pressure modulates intervertebral disc cell survival and extracellular matrix homeostasis via regulating hippo-YAP/TAZ pathway. *Stem Cells International*. 2021;2021:5626487.
7. Purmessur D, Guterl CC, Cho SK, et al. Dynamic pressurization induces transition of notochordal cells to a mature phenotype while retaining production of important patterning ligands from development. *Arthritis Res Ther*. 2013;15(5):1-14.
8. Kanda Y, Yurube T, Morita Y, et al. Delayed notochordal cell disappearance through integrin α5β1 mechanotransduction during ex-vivo dynamic loading-induced intervertebral disc degeneration. *J Orthop Res*. 2021;39(9):1933-1944.
9. Smolders LA, Bergknut N, Grinwis GC, et al. Intervertebral disc degeneration in the dog. Part 2: chondrodystrophic and non-chondrodystrophic breeds. *Vet J*. 2013;195(3):292-299.
10. Arkesteijn IT, Smolders LA, Spillekom S, et al. Effect of coculturing canine notochordal, nucleus pulposus and mesenchymal stromal cells for intervertebral disc regeneration. *Arthritis Res Ther*. 2015;17(1):1-12.
11. Omlor G, Nerlich A, Tirlapur U, Urban J, Guehring T. Loss of notochordal cell phenotype in 3D-cell cultures: implications for disc physiology and disc repair. *Arch Orthop Trauma Surg*. 2014;134(12):1673-1681.
12. Korecki CL, Taboas JM, Tuan RS, Iatridis JC. Notochordal cell conditioned medium stimulates mesenchymal stem cell differentiation toward a young nucleus pulposus phenotype. *Stem Cell Research & Therapy*. 2010;1(2):1-9.
13. de Vries SA, van Doeselaar M, Meij BP, Tryfonidou MA, Ito K. The stimulatory effect of notochordal cell-conditioned medium in a nucleus pulposus explant culture. *Tissue Eng Part A*. 2016;22(1–2):103-110.
14. Bach FC, de Vries S, Riemers FM, et al. Soluble and pelletable factors in porcine, canine and human notochordal cell-conditioned medium: implications for IVD regeneration. *Eur Cell Mater*. 2016;32:163-180.
15. Bach FC, Tellegen AR, Beukers M, et al. Biologic canine and human intervertebral disc repair by notochordal cell-derived matrix: from bench towards bedside. *Oncotarget*. 2018;9(41):26507-26526.
16. Bach FC, Poramba-Liyanage DW, Riemers FM, et al. Notochordal cell-based treatment strategies and their potential in intervertebral disc regeneration. *Frontiers in Cell and Developmental Biology*. 2022;9:780749.
17. Matta A, Karim MZ, Isenman DE, Erwin WM. Molecular therapy for degenerative disc disease: clues from secretome analysis of the notochordal cell-rich nucleus pulposus. *Sci Rep*. 2017;7:45623.
18. Varki A, Cummings RD, Esko JD, et al., eds. Essentials of glycobiology. *Cold Spring Harbor*. 3rd ed. Cold Spring Harbor Laboratory Press; 2017.
19. Ertunc N, Sato C, Kitajima K. Sialic acid sulfation is induced by the antibiotic treatment in mammalian cells. *Bioscience Biotechnology Biochemistry*. 2020;84(11):2311-2318.
20. Malisan F, Franchi L, Tomassini B, et al. Acetylation suppresses the proapoptotic activity of GD3 ganglioside. *J Exp Med*. 2002;196(12):1535-1541.
21. Rebelo AL, Gubinelli F, Roost P, et al. Complete spatial characterisation of N-glycosylation upon striatal neuroinflammation in the rodent brain. *J Neuroinflammation*. 2021;18(1):116.
22. Wang X, Inoue S, Gu J, et al. Dysregulation of TGF-β1 receptor activation leads to abnormal lung development and emphysema-like phenotype in core fucose-deficient mice. *Proc Natl Acad Sci*. 2005;102(44):15791-15796.
23. Zhang Z, Westhrin M, Bondt A, Wuhrer M, Standal T, Holst S. Serum protein N-glycosylation changes in multiple myeloma. *Biochim Biophys Acta Gen Subj*. 2019;1863(5):960-970.
24. Vanhooren V, Laroy W, Libert C, Chen C. N-glycan profiling in the study of human aging. *Biogerontology*. 2008;9(5):351-356.
25. Royle L, Campbell MP, Radcliffe CM, et al. HPLC-based analysis of serum N-glycans on a 96-well plate platform with dedicated database software. *Anal Biochem*. 2008;376(1):1-12.
26. Saldova R, Asadi Shehni A, Haakensen VD, et al. Association of N-glycosylation with breast carcinoma and systemic features using high-resolution quantitative UPLC. *J Proteome Res*. 2014;13(5):2314-2327.
27. Royle L, Radcliffe CM, Dwek RA, Rudd PM. Detailed structural analysis of N-glycans released from glycoproteins in SDS-PAGE gel bands using HPLC combined with exoglycosidase array digestions. *Glycobiology Protocols*. Springer; 2006:125-143.
28. Ludger. Product guide for LudgerTagTM DMB sialic acid release and labelling kit. 2017.
29. Wilkinson H, Thomsson KA, Rebelo AL, et al. The O-glycome of human nigrostriatal tissue and its alteration in Parkinson's disease. *J Proteome Res*. 2021;20(8):3913-3924.
30. Samal J, Saldova R, Rudd PM, Pandit A, O'Flaherty R. Region-specific characterization of N-glycans in the striatum

and substantia nigra of an adult rodent brain. *Anal Chem*. 2020;92(19):12842-12851.
31. Damerell D, Ceroni A, Maass K, Ranzinger R, Dell A, Haslam SM. The GlycanBuilder and GlycoWorkbench glycoinformatics tools: updates and new developments. *Biol Chem*. 2012;393(11):1357-1362.
32. Tateno H, Nakamura-Tsuruta S, Hirabayashi J. Comparative analysis of core-fucose-binding lectins from Lens culinaris and Pisum sativum using frontal affinity chromatography. *Glycobiology*. 2009;19(5):527-536.
33. de Vries S, Doeselaar MV, Meij B, Tryfonidou M, Ito K. Notochordal cell matrix as a therapeutic agent for intervertebral disc regeneration. *Tissue Eng Part A*. 2019;25(11–12):830-841.
34. Patil P, Dong Q, Wang D, et al. Systemic clearance of p16INK4a-positive senescent cells mitigates age-associated intervertebral disc degeneration. *Aging Cell*. 2019;18(3):e12927.
35. Zhong J, Chen J, Oyekan AA, et al. Ionizing radiation induces disc annulus fibrosus senescence and matrix catabolism via MMP-mediated pathways. *Int J Mol Sci*. 2022;23(7):4014.
36. Kim HI, Saldova R, Park JH, et al. The presence of outer arm fucose residues on the N-glycans of tissue inhibitor of metalloproteinases-1 reduces its activity. *J Proteome Res*. 2013;12(8):3547-3560.
37. Smolders LA, Meij BP, Onis D, et al. Gene expression profiling of early intervertebral disc degeneration reveals a down-regulation of canonical Wnt signaling and caveolin-1 expression: implications for development of regenerative strategies. *Arthritis Res Ther*. 2013;15(1):1-19.
38. Franzka P, Krüger L, Schurig MK, et al. Altered glycosylation in the aging heart. *Front Mol Biosci*. 2021;8:673044.
39. Ruhaak LR, Uh H-W, Beekman M, et al. Plasma protein N-glycan profiles are associated with calendar age, familial longevity and health. *J Proteome Res*. 2011;10(4):1667-1674.
40. Do KT, Chow LQM, Reckamp K, et al. First-in-human, first-in-class, phase I trial of the fucosylation inhibitor SGN-2FF in patients with advanced solid tumors. *Oncologist*. 2021;26(11):925-e1918.
41. Lattová E, Skřičková J, Hausnerová J, et al. N-glycan profiling of lung adenocarcinoma in patients at different stages of disease. *Mod Pathol*. 2020;33(6):1146-1156.
42. Agrawal P, Fontanals-Cirera B, Sokolova E, et al. A systems biology approach identifies FUT8 as a driver of melanoma metastasis. *Cancer Cell*. 2017;31(6):804-819. e7.
43. Li J, Jia L, Hao Z, et al. Site-specific N-glycoproteomic analysis reveals upregulated sialylation and core fucosylation during transient regeneration loss in neonatal mouse hearts. *J Proteome Res*. 2020;19(8):3191-3200.
44. Sanda M, Ahn J, Kozlik P, Goldman R. Analysis of site and structure specific core fucosylation in liver disease progression using exoglycosidase-assisted data-independent LC-MS/MS. *bioRxiv*. 2020;11:23273.
45. Martin TC, Šimurina M, Ząbczyńska M, et al. Decreased immunoglobulin G core fucosylation, a player in antibody-dependent cell-mediated cytotoxicity, is associated with autoimmune thyroid diseases. *Mol Cell Proteomics*. 2020;19(5):774-792.
46. Osumi D, Takahashi M, Miyoshi E, et al. Core fucosylation of E-cadherin enhances cell–cell adhesion in human colon carcinoma WiDr cells. *Cancer Sci*. 2009;100(5):888-895.
47. Liang W, Mao S, Li M, et al. Ablation of core fucosylation attenuates the signal transduction via T cell receptor to suppress the T cell development. *Mol Immunol*. 2019;112:312-321.
48. García-García A, Serna S, Yang Z, et al. FUT8-directed core fucosylation of N-glycans is regulated by the glycan structure and protein environment. *ACS Catalysis*. 2021;11(15):9052-9065.
49. Cavdarli S, Dewald JH, Yamakawa N, et al. Identification of 9-O-acetyl-N-acetylneuraminic acid (Neu5, 9Ac 2) as main O-acetylated sialic acid species of GD2 in breast cancer cells. *Glycoconj J*. 2019;36(1):79-90.
50. Ghosh S, Bandyopadhyay S, Mukherjee K, et al. O-acetylation of sialic acids is required for the survival of lymphoblasts in childhood acute lymphoblastic leukemia (ALL). *Glycoconj J*. 2007;24(1):17-24.
51. Grabenstein S, Barnard KN, Anim M, et al. Deacetylated sialic acids modulates immune mediated cytotoxicity via the sialic acid-Siglec pathway. *Glycobiology*. 2021;31(10):1279-1294.
52. Rayat G, Rajotte R, Hering B, Binette T, Korbutt G. In vitro and in vivo expression of Galalpha-(1, 3) gal on porcine islet cells is age dependent. *J Endocrinol*. 2003;177(1):127-135.
53. Contessotto P, Ellis BW, Jin C, et al. Distinct glycosylation in membrane proteins within neonatal versus adult myocardial tissue. *Matrix Biol*. 2020;85-86:173-188.
54. Barrientos G, Habazin S, Novokmet M, Almousa Y, Lauc G, Conrad ML. Changes in subclass-specific IgG fc glycosylation associated with the postnatal maturation of the murine immune system. *Sci Rep*. 2020;10(1):1-10.
55. Oriol R, Ye Y, Koren E, Cooper D. Carbohydrate antigens of pig tissues reacting with human natural antibodies as potential targets for hyperacute vascular rejection in pig-to-man organ xenotransplantation. *Transplantation*. 1993;56(6):1433-1442.
56. Wilson JM, Schuyler AJ, Workman L, et al. Investigation into the α-gal syndrome: characteristics of 261 children and adults reporting red meat allergy. The journal of allergy and clinical immunology. *In Pract*. 2019;7(7):2348-2358. e4.
57. Joyce K, Mohd Isa IL, Krouwels A, Creemers L, Devitt A, Pandit A. The role of altered glycosylation in human nucleus pulposus cells in inflammation and degeneration. *Eur Cell Mater*. 2021;41:401-420.
58. Nikolaou G, Zibis AH, Fyllos AH, et al. Detection of O-linked-N-acetylglucosamine modification and its associated enzymes in human degenerated intervertebral discs. *Asian Spine Journal*. 2017;11(6):863-869.
59. Collin EC, Kilcoyne M, White SJ, et al. Unique glycosignature for intervertebral disc and articular cartilage cells and tissues in immaturity and maturity. *Sci Rep*. 2016;6:23062.
60. Aguiar DJ, Johnson SL, Oegema TR Jr. Notochordal cells interact with nucleus pulposus cells: regulation of proteoglycan synthesis. *Exp Cell Res*. 1999;246(1):129-137.
61. Sinclair JW, Hoying DR, Bresciani E, et al. The Warburg effect is necessary to promote glycosylation in the blastema during zebrafish tail regeneration. *NPJ Regenerative Medicine*. 2021;6(1):1-16.
62. Oinam L, Changarathil G, Raja E, et al. Glycome profiling by lectin microarray reveals dynamic glycan alterations during epidermal stem cell aging. *Aging Cell*. 2020;19(8):e13190.

63. Fujita N, Miyamoto T, Imai J-i, et al. CD24 is expressed specifically in the nucleus pulposus of intervertebral discs. *Biochem Biophys Res Commun*. 2005;338(4):1890-1896.
64. Legler K, Rosprim R, Karius T, et al. Reduced mannosidase MAN1A1 expression leads to aberrant N-glycosylation and impaired survival in breast cancer. *Br J Cancer*. 2018;118(6):847-856.

SUPPORTING INFORMATION

Additional supporting information can be found online in the Supporting Information section at the end of this article.

How to cite this article: Günay B, Matthews E, Morgan J, Tryfonidou MA, Saldova R, Pandit A. An insight on the *N*-glycome of notochordal cell-rich porcine nucleus pulposus during maturation. *FASEB BioAdvances*. 2023;5:321-335. doi:10.1096/fba.2023-00011